Journal of Power Sources 205 (2012) 479–482

Contents lists available at SciVerse ScienceDirect

Journal of Power Sources

journal homepage: www.elsevier.com/locate/jpowsour

Short communication

Highly dispersed Ag nanoparticles (<10 nm) deposited on nanocrystalline $Li_4Ti_5O_{12}$ demonstrating high-rate charge/discharge capability for lithium-ion battery

Zhimin Liu [a], Naiqing Zhang [b,c], Zhijun Wang [a], Kening Sun [b,c,*]

[a] Department of Chemistry, Harbin Institute of Technology, Harbin 150001, PR China
[b] Academy of Fundamental and Interdisciplinary Sciences, Harbin Institute of Technology, Harbin 150001, PR China
[c] State Key Laboratory of Urban Water Resource and Environment, Harbin Institute of Technology, Harbin 150090, PR China

ARTICLE INFO

Article history:
Received 10 December 2011
Received in revised form 9 January 2012
Accepted 10 January 2012
Available online 18 January 2012

Keywords:
Lithium-ion battery
Anode
$Li_4Ti_5O_{12}$/Ag composite
High-rate
Electroless deposition

ABSTRACT

A $Li_4Ti_5O_{12}$ (LTO)/Ag composite is prepared via a facile electroless deposition (ED) process, and the electrochemical performance is examined for lithium-ion battery application. The nanosized Ag particles (<10 nm) are well dispersed on the surface of the nanocrystalline LTO (~90 nm). The LTO/Ag nanocomposite displays an excellent high-rate capacity of 131 mAh g^{-1} at 30 C within the voltage range of 1–2.5 V (versus Li^+/Li). Furthermore, the nanocomposite also exhibits excellent cycle stability, retaining over 98% of its initial capacity after 120 charge/discharge cycles at varying rates.

1. Introduction

Recently, considerable efforts have been made to develop high performance lithium-ion batteries (LIBs) for new applications including electric vehicles (EVs) and stationary power storage devices [1,2]. Spinel $Li_4Ti_5O_{12}$ (LTO) is an attractive negative electrode material that offers better safety and greater Li-ion intercalation and deintercalation reversibility than current commercially used materials and has been studied extensively over the past several years [3,4]. LTO displays a plateau in the Li insertion potential at approximately 1.55 V (versus Li^+/Li) [5], thus enabling LTO electrode to overcome many critical issues caused by undesirable electrolyte decomposition that occurs at reductive potential below 1 V (versus Li^+/Li). Furthermore, LTO displays excellent durability due to negligible volume expansion/contraction (<1%) compared to graphite, which experiences approximately 13% volume change during a full charge/discharge cycle [6–8].

Despite its many advantages, LTO suffers from low electrical conductivity (10^{-13} S cm^{-1}), thus resulting in poor electrochemical rate performance [9] and limiting its wide practical application. To overcome this issue, many efforts have been taken to ameliorate the rate capability of LTO, including developing nanostructures [10,11], metal doping [12] and surface modification with carbon [13] or other metals [14,15]. Although there have been many research efforts to develop nano-sized materials and carbon/LTO composites, both of them suffer from low packing density that ultimately results in low volumetric power density [16].

Comparatively, coating LTO electrode materials with metal nanoparticles has been proved to be an effective method of increasing the electronic conductivity while not decreasing the volumetric power density. In the past few years, several studies have been reported that depositing (mixing) silver on (with) electrode materials (such as $LiFePO_4$ [17], $LiCoO_2$ [18], $LiMn_2O_4$ [19] and $Li_4Ti_5O_{12}$ [20]) could greatly enhance the electronic conductivity as well as improving the high-rate capability and cycling stability. However, in these studies [17–20], active-material/Ag composites were obtained through direct mixing or thermal decomposition of precursors, which would induce growth or agglomeration of Ag particles. In this research, we deposit highly dispersed Ag nanoparticles (<10 nm) on nanocrystalline LTO via a simple electroless deposition (ED) method. The as-prepared nanocrystalline LTO/Ag is tested as anode material for lithium-ion battery and exhibits high reversible capacity and high-rate capability with good cycling performance.

* Corresponding author at: Academy of Fundamental and Interdisciplinary Sciences, Harbin Institute of Technology, Harbin 150001, PR China.
Tel.: +86 451 8641 2153; fax: +86 451 8641 2153.
E-mail address: keningsun@yahoo.com.cn (K. Sun).

0378-7753/$ – see front matter © 2012 Elsevier B.V. All rights reserved.
doi:10.1016/j.jpowsour.2012.01.068

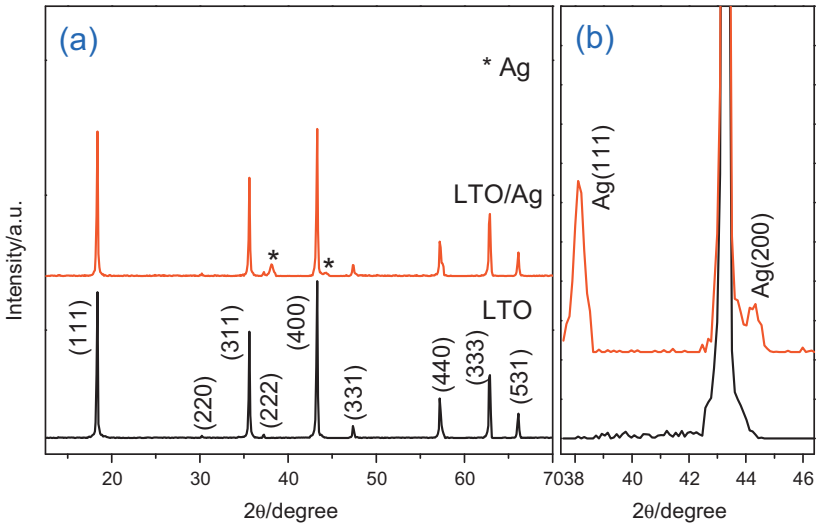

Fig. 1. (a) XRD patterns of pristine LTO and LTO/Ag composite; (b) local view of (a) in the 2θ range of 37.6–50°.

2. Experimental

The synthesis of the pristine LTO powder was described in our previous paper [21]. Briefly, we synthesized high-crystalline LTO via sol–gel process by employing a nonionic surfactant (EO)20(PO)70(EO)20 tri-block copolymer (pluronic P123) as the chelating agent. Nanosized Ag was deposited on LTO particles through a facile ED approach. Firstly, NH_3H_2O was dropped into an $AgNO_3$ solution (0.01 mol L^{-1}) until the white deposit disappeared. A transparent solution was therefore obtained on the basis of the following reaction:

$$Ag^+ + NH_3 \rightarrow Ag(NH_3)^+ \quad (1)$$

$$Ag(NH_3)^+ + NH_3 \rightarrow [Ag(NH_3)_2]^+ \quad (2)$$

Secondly, the above solution and dilute HCHO were added simultaneously into the suspension of LTO under vigorous

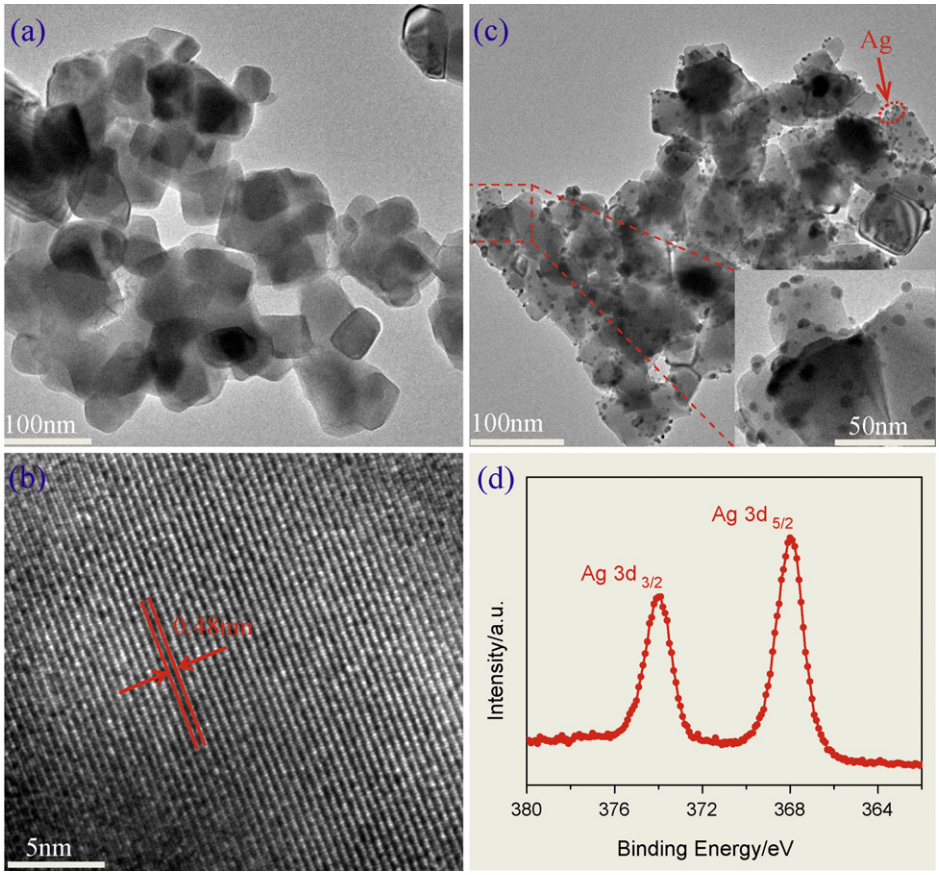

Fig. 2. Characterization of pristine LTO and LTO/Ag composite: (a) TEM image of pristine $Li_4Ti_5O_{12}$; (b) HRTEM image of pristine $Li_4Ti_5O_{12}$; (c) TEM image of $Li_4Ti_5O_{12}$/Ag composite (the inset shows the magnified image for $Li_4Ti_5O_{12}$); (d) Ag 3d spectra of the LTO/Ag composite.

magnetic stirring at room temperature. The following reaction took place:

$$2[Ag(NH_3)_2]^+ + 2OH^- + CH_3CHO \rightarrow 2Ag\downarrow + 3NH_3\uparrow + CH_3COO^- + H_2O + NH_4^+ \quad (3)$$

The weight ratio of $AgNO_3$ and LTO in the composite powders was estimated to be 6:94, corresponding to 3.6 wt.% Ag in the prepared LTO/Ag composite.

The resulting samples were characterized by means of X-ray diffraction (XRD, Rigaku D/max-γB) with monochromatic Cu Kα radiation at a scanning rate of 2° min^{-1} in the range of 10–70°. The microstructure of the powders was observed by a high resolution transmission electron microscopy (HRTEM, Hitachi 7650) operating at 300 kV. The electronic conductivity was measured by a four-point probe method and combined with a Keithley 2400 source meter. The conductivity measurement was performed on the powder sample which was pressed in the form of disk at 30 MPa with a diameter of 15 mm. The valence state was determined through X-ray photoelectron spectra (XPS) measurement (Thermofisher Scientific, K-Alpha) using monochromatic Al Kα (1486.6 eV) radiation under a vacuum of 1.0×10^{-8} mbar.

The anode films studied here were prepared by mixing the active materials, carbon black and polyvinylidene fluoride with a weight ratio of 8:1:1 in N-methyl pyrrolidinone. The slurry was coated onto an aluminum foil as the current collector by the "doctor blade" technique [22]. Both the LTO and LTO/Ag anodes were prepared with similar thicknesses of 30–35 μm and similar loadings of active material (~3 mg cm^{-2}). Coin type (CR2025) test cells were assembled in an argon-filled glove box (Mbraun) using two porous polypropylene films as a separator, 1 M $LiPF_6$ in ethylene carbonate, dimethyl carbonate and ethylmethyl carbonate (EC/DMC/EMC, 1:1:1, volume) as electrolyte, and Li foil as the counter and reference electrodes. Constant current charge/discharge measurement was performed at various rates within a voltage window of 1–2.5 V (versus Li^+/Li). Furthermore, the coulombic efficiency was calculated from the ratio of discharge capacity to charge capacity with the same current.

3. Results and discussion

The X-ray diffraction (XRD) spectra of LTO and the LTO/Ag composite are shown in Fig. 1a. All diffraction peaks are sharp and well defined, suggesting that both of the samples are highly crystallized. The pristine LTO can be completely indexed to the spinel structure (JCPDS Card No. 49-0207, S.G.: *Fd3m*). For the LTO/Ag spectra, several of the detected peaks can be ascribed to the detection of Ag, most noticeably the (1 1 1) plane at $2\theta = 38.1°$ and the (2 0 0) plane at $2\theta = 44.3°$ besides the main spinel structure, which can be observed clearly in the magnified profile (Fig. 1b). By using the Scherrer's equation, the average crystalline sizes of LTO and Ag are calculated to be 91 and 8.3 nm for the LTO/Ag composite, respectively.

Transmission electron microscopy (TEM) was then carried out to elucidate the microstructure of the as-derived LTO and LTO/Ag composite. The typical TEM image of LTO in Fig. 2a shows that the LTO has a cubic morphology with a uniform particle size distribution ranging from 80 to 100 nm. As depicted in the high-resolution TEM (HRTEM) image (Fig. 2b), the crystalline region with clear lattice fringes has an inter-planar spacing of approximately 0.48 nm, consistent with the (1 1 1) atomic planes of the spinel structure. The TEM images of the LTO/Ag composites are shown in Fig. 2c. It can be clearly observed that nanosized silver particles are uniformly distributed on the surface of the LTO particles. The magnified TEM image (inset of Fig. 2c) reveals that the particle size of Ag is less than 10 nm, which is in agreement with the XRD result. As revealed in XPS spectra (Fig. 2d), the binding energies of the LTO/Ag composite

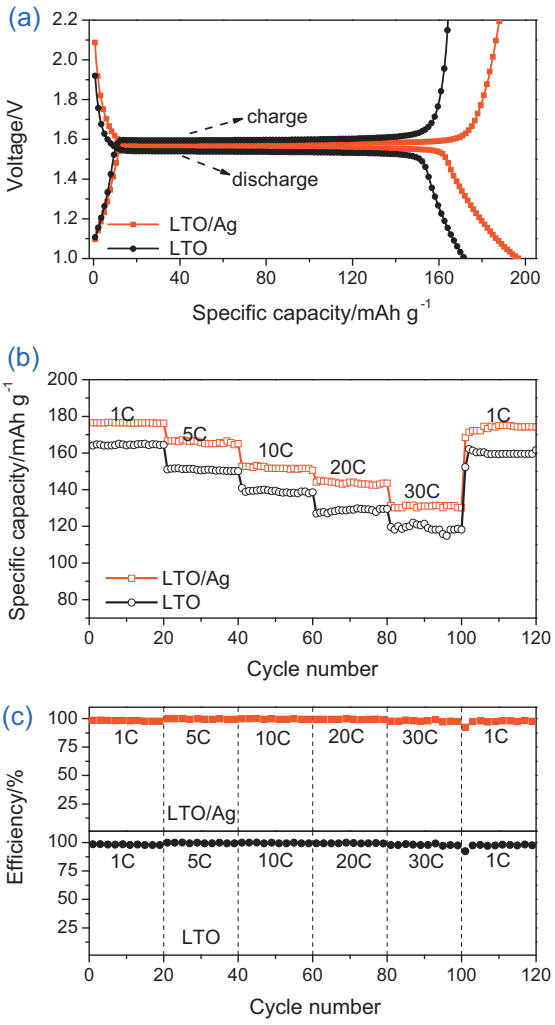

Fig. 3. (a) Voltage profiles of LTO and LTO/Ag composite between 1 V and 2.5 V at 0.2 C; (b) discharge capacity versus cycle number plot of LTO and LTO/Ag at different current rates (1–30 C); (c) coulombic efficiency versus cycle number plot of LTO and LTO/Ag at different current rates (1–30 C).

are 368 and 374 eV, corresponding to that of the Ag $3d_{5/2}$ and Ag $3d_{3/2}$, respectively. This result demonstrates that the Ag exists as an elementary substance in the LTO/Ag composite.

It was originally envisaged that these highly dispersed nanosized Ag particles could improve the electrical contact between LTO particles and current collector and may result in an improved discharge/charge performance of the LTO/Ag composite electrode. The electronic conductivity of the LTO/Ag composite was measured to be 4×10^{-5} S cm^{-1}, which was considerably higher than that of pristine $Li_4Ti_5O_{12}$ (8×10^{-7} S cm^{-1}). These results clearly demonstrate that the electronic conductivity was significantly increased by adding only a small amount of Ag (<3.6 wt.%), and is most likely due to the small size and fine dispersion of the Ag particles.

Fig. 3a shows the initial charge and discharge curves of LTO and LTO/Ag composite tested at the 0.2 C rate (34 mA g^{-1}). It can be observed that the pristine LTO and LTO/Ag composite have similar charge and discharge plateaus, indicating that the addition of Ag does not affect the electrochemical reaction process of LTO. Furthermore, the voltage separation (0.018 V) between the charge and discharge plateau potentials of LTO/Ag is smaller than that of LTO (0.057 V), demonstrating that the polarization of LTO/Ag is lower than that of LTO. It is also observed that the charge/discharge capacity of LTO/Ag composite (195/191 mAh g^{-1}) is higher than that of LTO (175/171 mAh g^{-1}) when tested under the same current

density. This result shows that the addition of Ag has significant positive impact on the charge/discharge capacity of LTO. To evaluate the high-rate performance of the LTO/Ag composite and LTO, the rate capabilities with charge/discharge rates increasing stepwise from 1 C to 30 C were measured. For each rate stage the cell was cycled for 20 times. As shown in Fig. 3b, the specific capacities of the LTO/Ag composite are superior to that of LTO at all charge/discharge rates. The relative increase in specific capacity was especially larger at higher rates. For instance, at a rate of 30 C (2 min for complete charge/discharge), the specific capacity of the LTO/Ag composite is 131 mAh g^{-1}, which is significantly greater than the specific capacity (114 mAh g^{-1}) of pristine LTO. The LTO/Ag composite and pristine LTO exhibit excellent cyclability, retaining over 98% of the initial capacity after 120 variational cycles. Both the rate capability and cycling performance of our LTO/Ag composite are significantly improved when compared with previous results from other literatures [10–15]. Furthermore, the coulombic efficiencies of the LTO/Ag composite and LTO at various charge/discharge rates approach 100% for each cycle. These results confirm that the incorporation of Ag nanoparticles is an effective method of increasing the conductivity of the LTO/Ag composite electrode and can greatly enhance the electron transport during the electrochemical lithium insertion/extraction reaction, which leads to significant improvement in the electrochemical performance.

4. Conclusions

To summarize, we have developed a facile method using electroless deposition to prepare LTO/Ag composite anode material for lithium-ion battery. The nanosized Ag particles (<10 nm) are well dispersed on the nanocrystalline LTO (~90 nm) and significantly improve the electronic conductivity of LTO. Electrochemical characterization of the LTO/Ag nanocomposite exhibits excellent charge/discharge capacities (195/191 mAh g^{-1}) at 0.2 C and high-rate capacity of 131 mAh g^{-1} at 30 C. This novel LTO/Ag composite with high reversible capacity, high-rate capability and excellent cyclic stability has been shown to be an excellent potential candidate as anode material for LIB.

Acknowledgements

This work is funded by National Natural Science Foundation of China (No. 20906015), Laboratory of Urban Water Resource and Environment, Harbin Institute of Technology (No. 2010QN08).

References

[1] M. Armand, J.M. Tarascon, Nature 451 (2008) 652.
[2] X.L. Wu, L.Y. Jiang, F.F. Cao, Y.G. Guo, L.J. Wan, Adv. Mater. 21 (2009) 2710.
[3] Z. Yang, D. Choi, S. Kerisit, K.M. Rosso, D. Wang, J. Zhang, G. Graff, J. Liu, J. Power Sources 192 (2009) 588.
[4] V. Etacheri, R. Marom, R. Elazari, G. Salitra, D. Aurbach, Energy Environ. Sci. 4 (2011) 3243.
[5] K. Zaghib, M. Simoneau, M. Armand, M. Gauthier, J. Power Sources 81 (1999) 300.
[6] T. Ohzuku, A. Ueda, N. Yamamoto, J. Electrochem. Soc. 142 (1995) 1431.
[7] K. Ariyoshi, R. Yamato, T. Ohzuku, Electrochim. Acta 51 (2005) 1125.
[8] Y. Koyama, T.E. Chin, U. Rhyner, R.K. Holman, S.R. Hall, Y.M. Chiang, Adv. Funct. Mater. 16 (2006) 492.
[9] S. Scharner, W. Weppner, P. Schmid-Beurmann, J. Electrochem. Soc. 146 (1999) 857.
[10] Y.F. Tang, L. Yang, Z. Qiu, J.S. Huang, Electrochem. Commun. 10 (2008) 1513.
[11] A.S. Prakash, P. Manikandan, K. Ramesha, M. Sathiya, J.-M. Tarascon, A.K. Shukla, Chem. Mater. 22 (2010) 2857.
[12] H. Ge, N. Li, D. Li, C. Dai, D. Wang, Electrochem. Commun. 10 (2008) 1031.
[13] L. Shen, C. Yuan, H. Luo, X. Zhang, K. Xua, F. Zhang, J. Mater. Chem. 21 (2011) 761.
[14] M. Mokhlesur Rahman, J.-Z. Wang, M.F. Hassan, D. Wexler, H.K. Liu, Adv. Energy Mater. 1 (2011) 212.
[15] L. Zhao, Y.-S. Hu, H. Li, Z. Wang, L. Chen, Adv. Mater. 23 (2011) 1385.
[16] K. Amine, I. Belharouak, Z. Chen, T. Tran, H. Yumoto, N. Ota, S.T. Myung, Y.K. Sun, Adv. Mater. 22 (2010) 3052.
[17] C.H. Mi, Y.X. Cao, X.G. Zhang, X.B. Zhao, H.L. Li, Powder Technol. 181 (2008) 301.
[18] S.H. Huang, Z.Y. Wen, X.L. Yang, Z.H. Gu, X.H. Xu, J. Power Sources 148 (2005) 72.
[19] W.J. Zhou, B.L. He, H.L. Li, Mater. Res. Bull. 43 (2008) 2285.
[20] S. Huang, Z. Wen, J. Zhang, Z. Gu, X. Xu, Solid State Ionics 177 (2006) 851.
[21] N. Zhang, Z. Liu, T. Yang, C. Liao, Z. Wang, K. Sun, Electrochem. Commun. 13 (2011) 654.
[22] T.Y. Yang, K.N. Sun, Z.Y. Lei, N.Q. Zhang, Y. Lang, J. Alloys Compd. 502 (2010) 215.